REPORT DOCUMENTATION PAGE

Form Approved
OMB No. 0704-0188

1. REPORT DATE *(DD-MM-YYYY)*	2. REPORT TYPE	3. DATES COVERED *(From - To)*
7 May 2003	Technical Abstract	

4. TITLE AND SUBTITLE

Internal Energy Mode Relaxation in High Speed Continuum and Rarefied Flows

5a. CONTRACT NUMBER
F04611-99-C-0025

5b. GRANT NUMBER

5c. PROGRAM ELEMENT NUMBER

6. AUTHOR(S)

E. Josyula, D. Wadsworth

5d. PROJECT NUMBER
2308

5e. TASK NUMBER
M19B

5f. WORK UNIT NUMBER

7. PERFORMING ORGANIZATION NAME(S) AND ADDRESS(ES)

ERC, Inc.
10 E. Saturn Blvd.
Edwards AFB CA 93524-7680

8. PERFORMING ORGANIZATION REPORT NUMBER

9. SPONSORING / MONITORING AGENCY NAME(S) AND ADDRESS(ES)

Air Force Research Laboratory (AFMC)
AFRL/PRS
5 Pollux Drive
Edwards AFB CA 93524-7048

10. SPONSOR/MONITOR'S ACRONYM(S)

11. SPONSOR/MONITOR'S NUMBER(S)
AFRL-PR-ED-AB-2003-123

12. DISTRIBUTION / AVAILABILITY STATEMENT

Approved for public release; distribution unlimited.

13. SUPPLEMENTARY NOTES

14. ABSTRACT

15. SUBJECT TERMS

16. SECURITY CLASSIFICATION OF:			17. LIMITATION OF ABSTRACT	18. NUMBER OF PAGES	19a. NAME OF RESPONSIBLE PERSON
a. REPORT	b. ABSTRACT	c. THIS PAGE			Sheila Benner
Unclassified	Unclassified	Unclassified	A		19b. TELEPHONE NUMBER *(include area code)* (661) 275-5693

Standard Form 298 (Rev. 8-98)
Prescribed by ANSI Std. 239.18

FILE

MEMORANDUM FOR PRS (In-House Contractor Publication)

FROM: PROI (STINFO) 07 May 2003

SUBJECT: Authorization for Release of Technical Information, Control Number: **AFRL-PR-ED-AB-2003-123**
E. Josyula (WPAFB); D. Wadsworth (AFRL/ERC), "Internal Energy Mode Relaxation in High Speed Continuum and Rarefied Flows" (abstract only)

915

42nd AIAA Aerospace Sciences Meeting & Exhibit **(Statement A)**
(Reno, NV, 5-8 January 2004) (Deadline: 08 May 2003)

Proposed Abstract of

INTERNAL ENERGY MODE RELAXATION IN HIGH SPEED CONTINUUM AND RAREFIED FLOWS

By Eswar Josyula* and Dean C. Wadsworth†

Introduction

The presence of shock waves in high speed flow of a polyatomic gas presents considerable difficulties for accurate numerical simulation of the flowfield. The shock wave redistributes the high kinetic energy of the oncoming flow into various internal energy modes, which relax relatively slowly, leading to significant chemical and thermal nonequilibrium in the stagnation region. In the gas kinetic description, intermolecular collisions change the translational, rotational, vibrational, and electronic energies of the collision partners. The probabilities or effective cross sections of these elementary processes differ significantly, giving rise to widely separate relaxation times for the internal modes. Thus it becomes important to account for the rates of relaxation processes to predict the nonequilibrium behavior of these kinds of flows. The continuum description is well suited at lower altitudes of the flight regime for the prediction of aerodynamic loads and heating rates on the thermal protection systems. However, at high altitudes and associated low densities the larger mean free path invalidates

*Research Aerospace Engineer, Air Force Research Laboratory, 2210 Eighth Street, Wright-Patterson AFB, OH 45433. Associate Fellow AIAA

†Research Scientist, ERC, Inc., 10 E. Saturn Blvd., Edwards Air Force Base, CA 93524. Member AIAA

the continuum assumption and the rarefied solution approaches are necessary [1]. Among the solution approaches in hypersonic rarefied flows, the Direct Simulation Monte Carlo (DSMC) method is widely used [2].

In the continuum approach the Navier-Stokes equations consist of reaction probabilities for quantifying the thermal and chemical nonequilibrium effects. These are typically temperature-dependent, though the concept of temperature in a nonequilibrium flow is ill-defined. In the DSMC method, however, the internal energy relaxation occurs as a consequence of intermolecular collisions. This requires knowledge of the level-to-level cross-sections for internal energy modes and the energy-dependent cross-sections of chemical reactions. Recent studies [3, 4] were aimed at finding a consistent way of interpreting nonequilibrium in both the approaches. The work of Ref. [4] developed an exact relationship that connects the vibrational relaxation number used in DSMC method to the continuum method. A meaningful comparison of the reaction probabilities and cross-sections is critical to the development of numerical predictive tools that span the continuum and rarefied regimes. It is one of the objectives of the proposed study.

The internal energy mode relaxation in the shock wave structure was studied using continuum and rarefied approaches by various investigators. See for example, Refs. [5, 6]. The advantage of the shock structure problems is that it does not involve the nonequilibrium effects of gas-surface interactions, an area of research not considered in the proposed paper. Numerical experiments performed by Pham-Van-Diep, et al. [7] in testing continuum descriptions showed that the continuum solutions of the shock structure in a monatomic gas were able to match the rarefied solution at a Mach number of 1.2. At higher Mach numbers the solutions obtained with continuum approach do not match those by the DSMC method. The proposed study will address the inconsistencies in relaxation mechanisms implemented in Continuum and DSMC codes.

The rotational energy relaxation in shock structures of Nitrogen was studied using

Burnett equations by Lumpkin, et al. [8]. The model was validated with experiment up to Mach 6. In the vibrational energy relaxation implemented in the continuum approach of Josyula [9] the master equations were coupled to the fluid dynamic equations to model the nonequilibrium flow physics in Hypersonic flow. These two modeling approaches will be used in the present study to compare with results obtained by the DSMC code.

Analysis

This section gives the governing Navier-Stokes equations used for coupling to the Lumped Landau-Teller Vibrational Relaxation Model (LLTR) and Discrete State Kinetic Relaxation Model (DSKR).

The global conservation equations in mass-averaged velocity form are shown below:

$$\frac{\partial}{\partial t}(\rho_v) + \nabla \cdot [\rho_v(\vec{\mathbf{u}} + \vec{\mathbf{u}}_{\mathbf{N_2}} + \vec{\mathbf{u}}_{\mathbf{vN_2}})] = \dot{\omega}_{\mathbf{v}} \quad v=0,1,... \tag{1}$$

$$\frac{\partial}{\partial t}(\rho_s) + \nabla \cdot [\rho_s(\vec{\mathbf{u}} + \vec{\mathbf{u}}_{\mathbf{s}})] = \dot{\omega}_{\mathbf{s}} \tag{2}$$

$$\frac{\partial}{\partial t}(\rho\vec{\mathbf{u}}) + \nabla \cdot (\rho\vec{\mathbf{u}}\vec{\mathbf{u}} + \tilde{\tau}) = 0 \tag{3}$$

$$\frac{\partial}{\partial t}(\rho e_{vib}) + \nabla \cdot [\rho e_{vib}(\vec{\mathbf{u}} + \vec{\mathbf{u}}_{\mathbf{s}}) + \dot{q}_{vib}] = \rho\dot{\omega}_{vib} + e_{vib}\dot{\omega} + Q_{T-v} \tag{4}$$

$$\frac{\partial}{\partial t}(\rho e) + \nabla \cdot [\rho(e + p/\rho)\vec{\mathbf{u}} - (\sum \dot{q}_{vib} + \dot{q}_{trans}) + \sum(\rho_s h_s \vec{\mathbf{u}}_{\mathbf{s}}) - \vec{\mathbf{u}} \cdot \tilde{\tau}] = 0 \tag{5}$$

The conservation Equation (1) used in the DSKR code is written for mass density in quantum level v for diatomic nitrogen. The term $\vec{\mathbf{u}}_{\mathbf{N_2}}$ denotes the diffusion velocity of component N_2 of the gas mixture and $\vec{\mathbf{u}}_{\mathbf{vN_2}}$ is the diffusion velocity of level v relative to N_2 diffusion velocity. The source term $\dot{\omega}_v$ derived from the vibrational master equations is made up of the relevant energy exchange processes consisting of the V-T

and V-V reaction mechanisms. Of the three species (O_2, N_2, and O) considered for the air mixture in the DSKR code, only the species N_2 was treated as an anharmonic oscillator in the DSKR model with the following energy exchange mechanisms.

$$\dot{\omega}_v = (\dot{\rho}_{N_2-N_2})^{V-T} + (\dot{\rho}_{N_2-N_2})^{V-V} + (\dot{\rho}_{N_2-O_2})^{V-T} + (\dot{\rho}_{N_2-O})^{V-T} + (\dot{\rho}_{N_2\rightarrow N})^{diss} + (\dot{\rho}_{N\rightarrow N_2})^{recomb} \tag{6}$$

The density of molecular nitrogen is the sum of population densities in the various vibrational levels.

$$\rho_{N_2} = \sum_{v=0,1..} \rho_v \tag{7}$$

The mass conservation of species treated in the LLTR model is represented by Equation (2). The production of small amounts of atoms due to dissociation of molecules is included in the source term, $\dot{\omega}_s$. The term $\vec{\mathbf{u}}_\mathbf{s}$ denotes the diffusion velocity of component s of the gas mixture. The mixture density, ρ is the sum of the partial species densities,

$$\rho = \rho_{N_2} + \rho_{O_2} + \rho_O + \rho_{NO} + \rho_N \tag{8}$$

For simulations in air, the maximum temperature of the shock was below 7,000 K, thereby necessitating the oxygen dissociation reaction in the DSKR code. Due to small amount of nitrogen dissociation and the difficulty of incorporating collision probabilities of additional species, only oxygen dissociation was considered in the DSKR model. However, the LLTR code considered N and NO also.

Equation (3) gives the conservation of total momentum. Equation (4) is the conservation equation for vibrational energy where Q_{T-v} denotes the energy exchange between the vibrational and translational modes. For diatomic nitrogen in the DSKR code, a separate vibrational conservation equation was not necessary as the vibrational energy was calculated at each quantum level, discussed later. The diatomic oxygen molecules in the DSKR code and all the species in the LLTR model were assumed as harmonic oscillators. Equation (4) was solved with a source term for the

V-T coupling, modeled according to the Landau-Teller [10, 11] form:

$$\dot{\omega}_{vib} = \frac{e^*_{vib_s} - e_{vib_s}}{\tau_s} \tag{9}$$

where e_{vib_s} is the vibrational energy of the molecular species s and $e^*_{vib_s}$ is the vibrational energy in thermal equilibrium at the local translational temperature, the relaxation time given by

$$\tau_s = \frac{\sum_s X_s}{\sum_s X_s / \tau_{LT}} \tag{10}$$

where X_s denotes the species mole fraction and τ_{LT} is the Landau-Teller inter-species relaxation times. τ_{LT} was computed using the expression developed by Millikan and White [12]. The vibrational temperature of molecular species s was determined by inverting the expression for the vibrational energy contained in a harmonic oscillator at the temperature, T_v,

$$e_{vib(s)} = \frac{R\Theta_{v(s)}}{e^{\Theta_{v(s)}/T_v} - 1} \tag{11}$$

where R is the species gas constant per unit mass. V-V exchanges were considered only between the nitrogen molecules in the DSKR model used to compare to the LLTR model; they were neglected for the oxygen molecules in the DSKR model and all the species in the LLTR model. The DSKR model incorporating the new vibration-dissociation coupling neglected V-V exchanges also. Equation (4) also includes terms for the conduction and diffusion of vibrational energy. The conservation of total energy is given by Equation (5) with heat conduction and species diffusion terms.

The kinetics of the particle exchanges among the quantum states of N_2 were simulated by the vibrational master equations. The population distributions were calculated by: [9]

$$\begin{aligned} \dot{\omega}_v &= \frac{1}{M}\left\{\sum_{v'}\left[k_{VT}(v' \rightarrow v)\rho_{v'}\rho - k_{VT}(v \rightarrow v')\rho_v\rho\right]\right. \\ &+ \left.\sum_{w}\left[k_{VV}(v', w' \rightarrow v, w)\rho_{v'}\rho_{w'} - k_{VV}(v, w \rightarrow v', w')\rho_v\rho_w\right]\right\} \end{aligned} \tag{12}$$

where only single quantum transitions have been considered. The equations governing the V-T reactions responsible for the variation of the particles distributed in the v^{th}

vibrational level of diatomic nitrogen are:

$$N_2(v) + M \rightleftharpoons N_2(v-1) + M \tag{13}$$

where M represents O_2, O, N_2. The equations governing the V-V processes in N_2 giving the reactions responsible for the variation of the particles distributed in the v^{th} vibrational level are:

$$N_2(v) + N_2(w) \rightleftharpoons N_2(v-1) + N_2(w+1) \tag{14}$$

For the kinetics of diatomic nitrogen, the present study used: (a) V-T forward rate coefficients calculated according to expressions proposed by Capitelli, et al. [13] and Billing and Fisher [14] and (b) V-V forward rates by Doroshenko, et al. [15]. The V-T forward rate coefficient for N_2-O collisions was from the work of Capitelli [16] which was based on Refs. [17] and [18]. Reverse rate coefficients were derived from detailed balance.

The vibrational energy of the N_2 molecule is given in terms of the quantum level energies by

$$e_{vib_{N2}} = \sum_{i=1,2,..} \frac{\rho_i}{\rho_{N2}} \epsilon_i \tag{15}$$

where the index i is used to denote the quantum level. In this equation, $\frac{\rho_i}{\rho_{N_2}}$ is the fractional population of the i^{th} vibrational level and ϵ_i the quantum level energy given by the third-order approximating formula:

$$\frac{\epsilon_i}{hc} = \omega_e(i-\frac{1}{2}) - \omega_e x_e(i-\frac{1}{2})^2 + \omega_e y_e(i-\frac{1}{2})^3 \quad i=1,2,...l+1 \tag{16}$$

The above equation represents anharmonic-oscillator behavior of the N_2 molecule, where h is the Planck's constant and c is the speed of light. The spectroscopic constants are given by, [19] ω_e=2358.57 cm^{-1}, $\omega_e x_e$=14.324 cm^{-1}, and $\omega_e y_e$=-0.00226 cm^{-1}. When i=45, the value of energy exceeds the N_2 dissociation energy, 9.62 eV. [20]

Numerical Procedure

In the continuum approach, the Roe approximate Riemann solver is implemented in finite volume formulation by computing the cell interface flux as a summation of wave speeds as described by Cinnella, et al. [21]. The second order spatial accuracy is obtained by employing the MUSCL approach in conjunction with the minmod limiter to reduce the solution to first order accuracy in the vicinity of strong shock waves, as described in the work of Josyula, et al [22]. The entropy correction for the Roe scheme is implemented as discussed in the Reference [22]. The viscous terms are evaluated using central differencing. An explicit predictor-corrector method is used to advance the solution in time. This approach was discussed for the flux-splitting option by MacCormack in Reference [23].

The rarefied approach uses the Direct Simulation Monte Carlo (DSMC) code developed by Wadsworth, et al. [24]. The code was used to study nonequilibrium flowfield applications and includes energy exchange mechanism for vibrational and rotational energy transfers.

Preliminary Results and Discussion

The Navier-Stokes continuum code, described above, using the perfect gas assumption was used to compute the internal structure of a shock wave. Comparisons were made for low Mach Number shock waves with (a) theoretically obtained Navier-Stokes solution, (b) available experimental data and (c) the results obtained by a DSMC code. These perfect gas computations and comparisons were made to establish a baseline for which the internal energy modes of rotational and vibrational mode relaxation will be computed in the proposed paper.

Figure 1 shows the comparison of flow parameters inside a Mach 2 shock wave using a perfect gas Navier-Stokes computational code and the exact Navier-Stokes

solution. For the perfect gas assumption, the agreement of both sets of results is excellent.

Experimental measurements reported by Sherman [25] inside the shock wave structure were used for comparison in the next figure. Temperature comparisons using the present Navier-Stokes computational code using the perfect gas assumption and the experimental data are shown in Fig. 2. The flow Mach number is 1.9 in air and the computed results are shown for three different bulk viscosity coefficients, $\lambda = -2/3\mu$, $\lambda = +4/3\mu$, and $\lambda = 2\mu$. The internal energy relaxation related to the bulk modulus does have a significant effect on the result. For the commonly used value of $\lambda = -2/3\mu$, the temperature is underpredicted for $M < 1$ and overpredicted for $M > 1$. Increasing the value of λ, however, compensates for this under- and overprediction. This signifies the importance of rotational and vibrational relaxation in the shock structure.

Figures 3 to 7 show the variation of pressure, density, temperature and velocity Argon shock structure using the perfect gas, Navier-Stokes code and DSMC method. The continuum calculations for Mach 1.2 (Fig. 3) match those obtained using the DSMC method. However, at a higher Mach number of 2 shown in Fig. 4, one can see the thicker shock profile for the pressure variation across the shock wave obtained by the DSMC code compared to the Navier-Stokes code. The mass density obtained by the DSMC, Fig. 5, shows the thicker shock thickness, the thickness slightly higher for $M > 1$. The temperature and velocity profiles of the continuum solutions, Fig. 6 and Fig. 7 show greater thickness in the region for $M < 1$.

References

[1] E.P. Muntz. Rarefied Gas Dynamics. *Annual Review of Fluid Mechanics*, 21:387–417, 1989.

[2] G.A. Bird. *Molecular Gas Dynamics and the Direct Simulation of Gas Flows.* Oxford University Press, inc., New York, 1994.

[3] M.S. Ivanov and S.F. Gimelshein. Computational Hypersonic Rarefied Flows. *Annual Review of Fluid Mechanics*, 30:469–505, 1998.

[4] N.E. Gimelshein, S.F. Gimelshein, and D.A. Levin. Vibrational Relaxation Rates in the Direct Simulation Monte Carlo Method. *Physics of Fluids*, 14(12):4452–4455, December 2002.

[5] D. Gilbarg and D. Paolucci. The Structure of Shock Waves in the Continuum Theory of Fluids. *Journal of Rational Mechanics and Analysis*, 2(4):617–642, 1953.

[6] G.A. Bird. The Velocity Distribution Function Within a Shock Wave. *Journal of Fluid Mechanics*, 30(3):479–487, 1967.

[7] G.C. Pham-Van-Diep, D.A. Erwin, and E.P. Muntz. Testing Continuum Descriptions of Low Mach Number Shock Structures. *Journal of Fluid Mechanics*, 232:403–413, 1991.

[8] F.E. Lumpkin III, D.R. Chapman, and C. Park. A new rotational relaxation model for use in hypersonic computational fluid mechanics. *AIAA Paper 89-1737*, 1989.

[9] E. Josyula. Computational Study of Vibrationally Relaxing Gas Past Blunt Body in Hypersonic Flows. *Journal of Thermophysics and Heat Transfer*, 14(1):18–26, January 2000.

[10] L. Landau and E. Teller. Zur Theorie der Schalldispersion. *Physikalische Zeitschrift der Sowjetunion*, 10(1):34–43, 1936.

[11] W.G. Vincenti and C.H. Kruger Jr. *Introduction to Physical Gas Dynamics.* John Wiley & Sons, 1967.

[12] R.C. Millikan and D.R. White. Systematics of Vibrational Relaxation. *Journal of Chemical Physics*, 39(12):3209–3213, 1963.

[13] M. Capitelli, C. Gorse, and G.D. Billing. V-V Pumping Up in Nonequilibrium Nitrogen: Effects on the Dissociation Rate. *Chemical Physics*, 52(3):299–304, 1980.

[14] G.D. Billing and E.R. Fisher. VV and VT Rate Coefficients in Diatomic Nitrogen by a Quantum Classical Model. *Chemical Physics*, 43(3):395–401, 1979.

[15] V.M. Doroshenko, N.N. Kudryavtsev, S.S. Novikov, and V.V. Smetanin. Effect of the Formation of Vibrationally Excited Nitrogen Molecules in Atomic Recombination in a Boundary Layer on the Heat Transfer. *High Temperature (USSR)*, 28(1):82–89, 1990.

[16] M. Capitelli, I. Armenise, and C. Gorse. State-to-State Approach in the Kinetics of Air Components Under Re-Entry Conditions. *Journal of Thermophysics and Heat Transfer*, 11(4):570–578, October 1997.

[17] G.D. Billing. VV and VT Rates in N_2-O_2 Collisions. *Chemical Physics*, 179(3):463–467, 1994.

[18] A.K. Mnatsakanyan and G.V. Naidis. The Vibrational-Energy Balance in a Discharge in Air. *High Temperature (USSR)*, 4(3):506–513, 1985.

[19] K.P. Huber and G. Herzberg. *Constants of Diatomic Molecules.* Van Nostrand Reinhold Company, New York, 1979.

[20] I. Armenise, M. Capitelli, R. Celiberto, G. Colonna, and C. Gorse. The Effect of N + N_2 Collisions on the Non-equilibrium Vibrational Distributions of Nitrogen under Reentry Conditions. *Chemical Physics Letters*, 227(1):157–163, 1994.

[21] P. Cinnella and B. Grossman. Upwind Techniques for Flows with Multiple Translational Temperatures . *AIAA Paper 90-1660*, June 1990.

[22] E. Josyula and J.S. Shang. Computation of Hypersonic Flowfields in Thermal and Chemical Nonequilibrium. *AIAA Paper 92-2874*, July 1992.

[23] R. MacCormack. Current Status of Numerical Solutions of the Navier-Stokes Equations. *AIAA Paper 85-0032*, 1985.

[24] D.C. Wadsworth, I.J. Wysong, and D.H. Campbell. Direct Simulation Monte Carlo Modeling for Non-Equilibrium Flowfield Applications. Technical Report PL-TR-97-3024, Air Force Research Laboratory, Edwards Air Force Base, CA, May 1999.

[25] F.S. Sherman. A low density wind-tunnel study of shock-wave structure and relaxation phenomena in gases. Technical Report Technical Note 3298, National Advisory Committee for Aeronautics, Washington, July 1955.

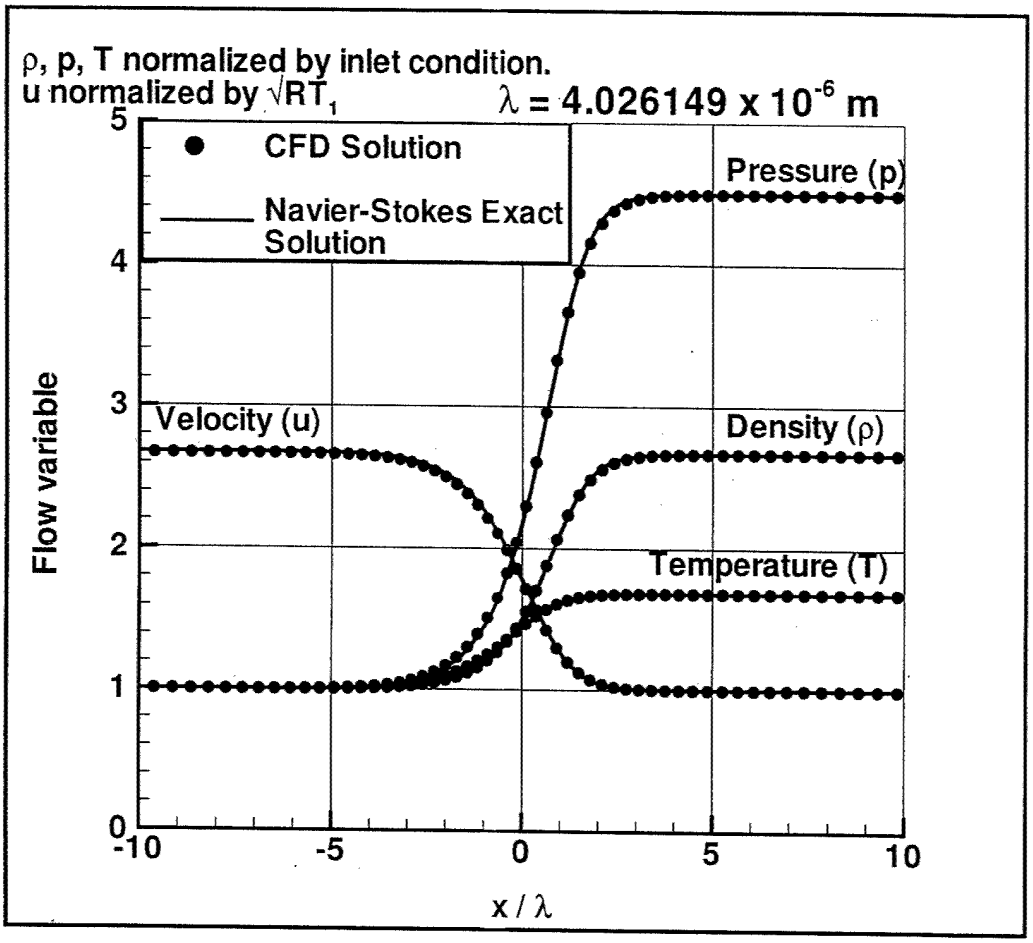

Figure 1: Comparison of flow parameters across shock wave in Mach 2 air flow between Navier-Stokes CFD calculation and exact solution

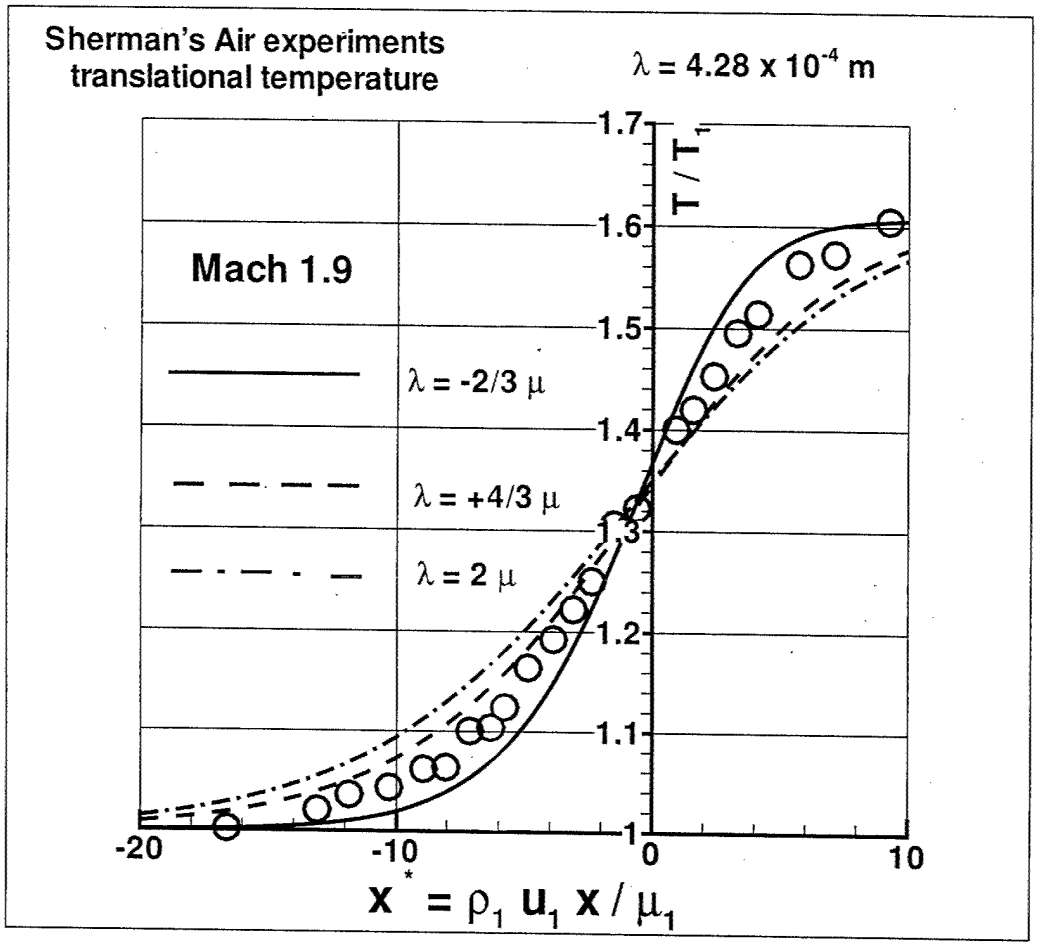

Figure 2: Comparison of flow parameters across shock wave in Mach 1.9 air flow between Navier-Stokes, perfect gas CFD solution and Experiment showing effect of varying the bulk viscosity in the Navier-Stokes equations

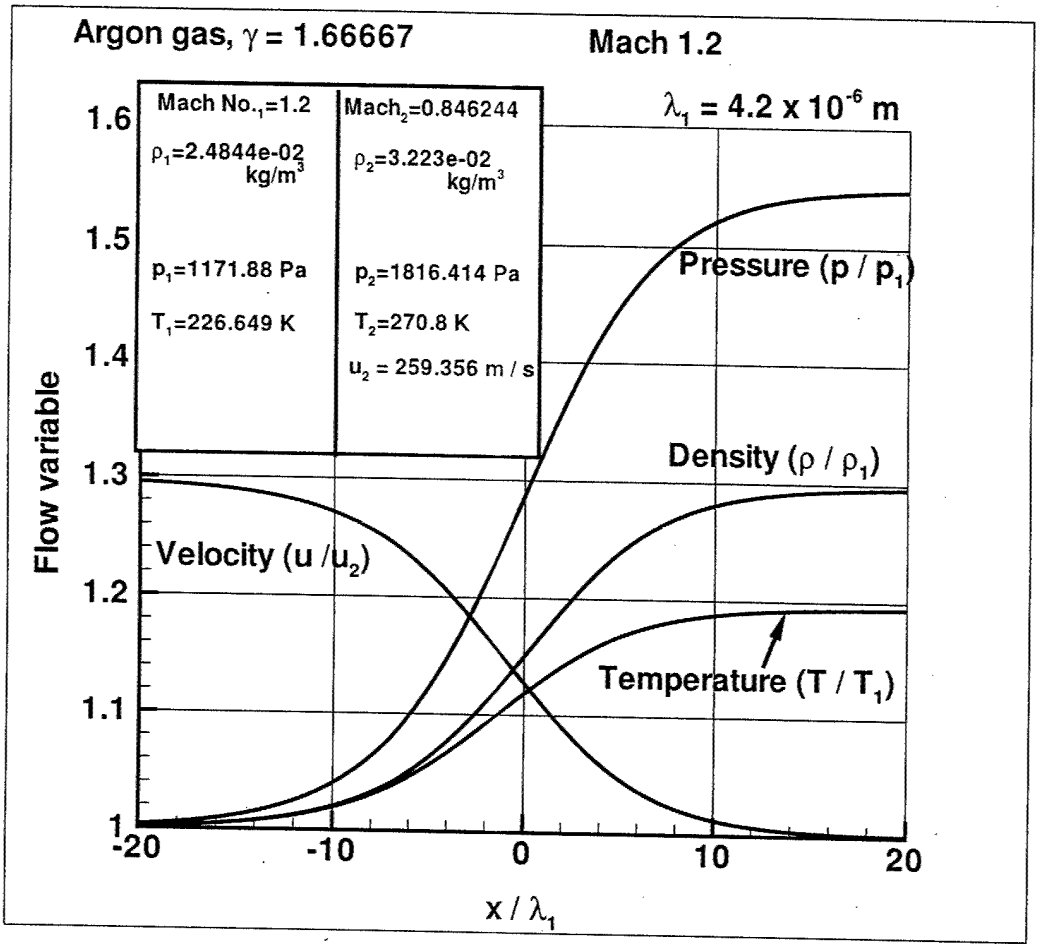

Figure 3: Variation of flow parameters across shock wave in Mach 1.2 Argon

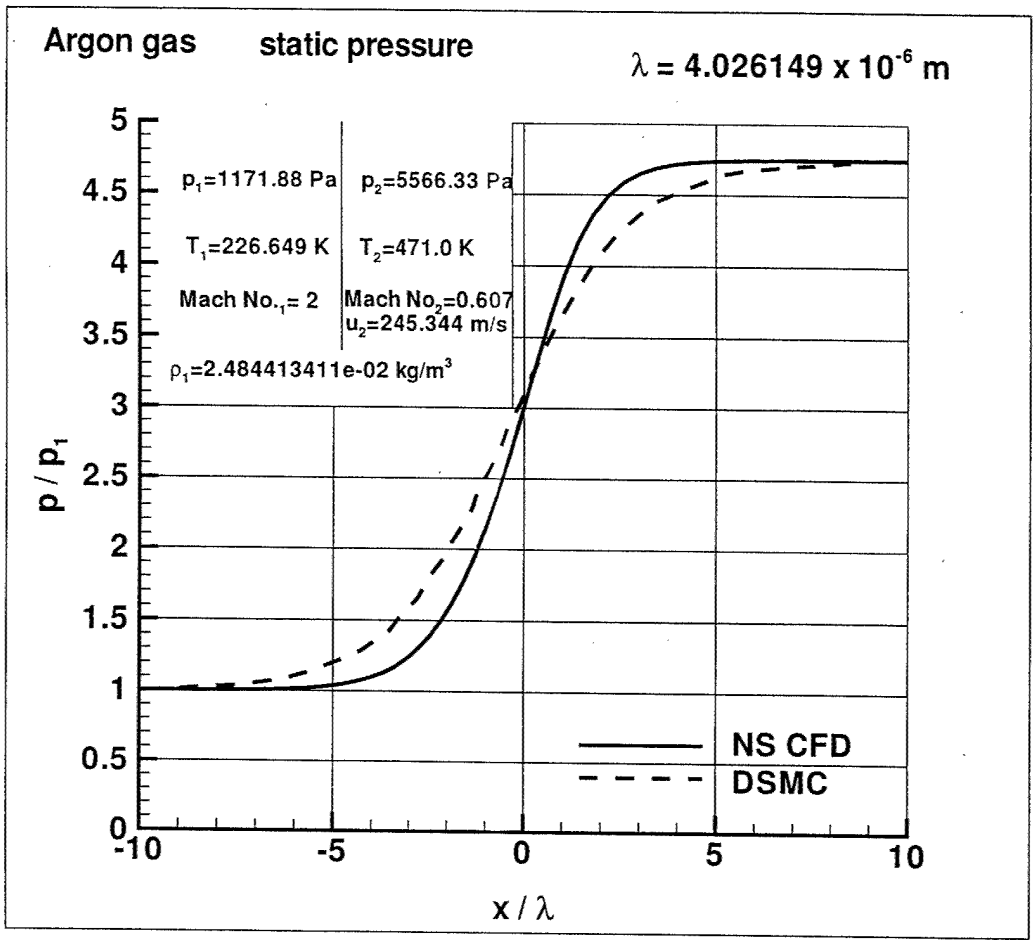

Figure 4: Comparison of static pressure across shock wave in Mach 2 argon flow between Navier-Stokes CFD solution and DSMC

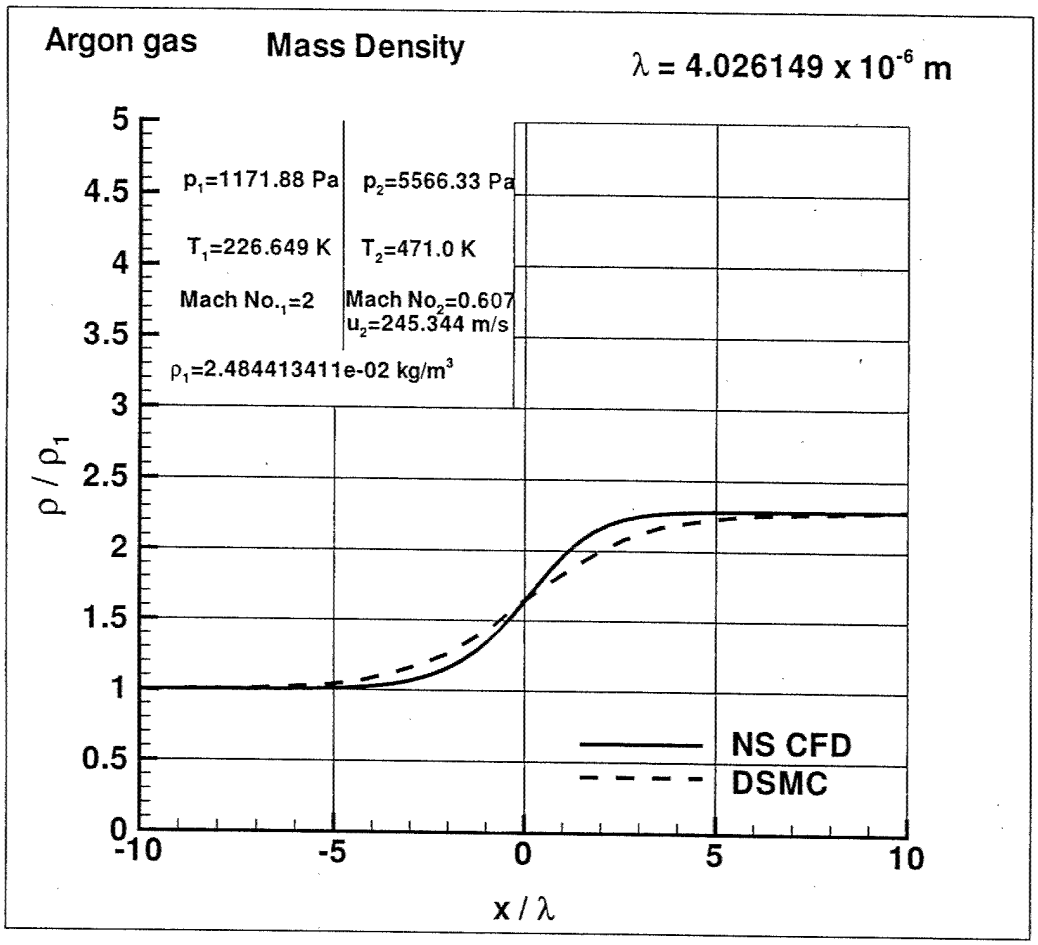

Figure 5: Comparison of mass density across shock wave in Mach 2 argon flow between Navier-Stokes CFD solution and DSMC

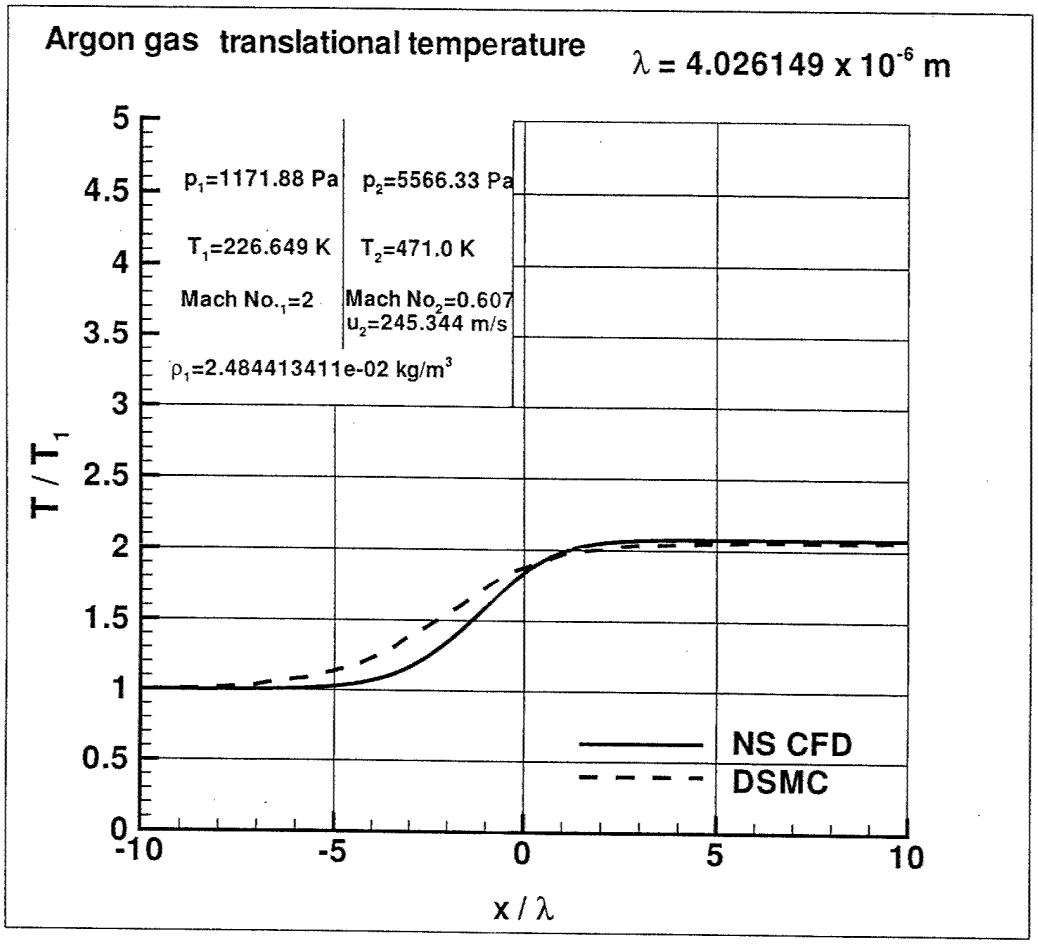

Figure 6: Comparison of temperature across shock wave in Mach 2 argon flow between Navier-Stokes CFD solution and DSMC

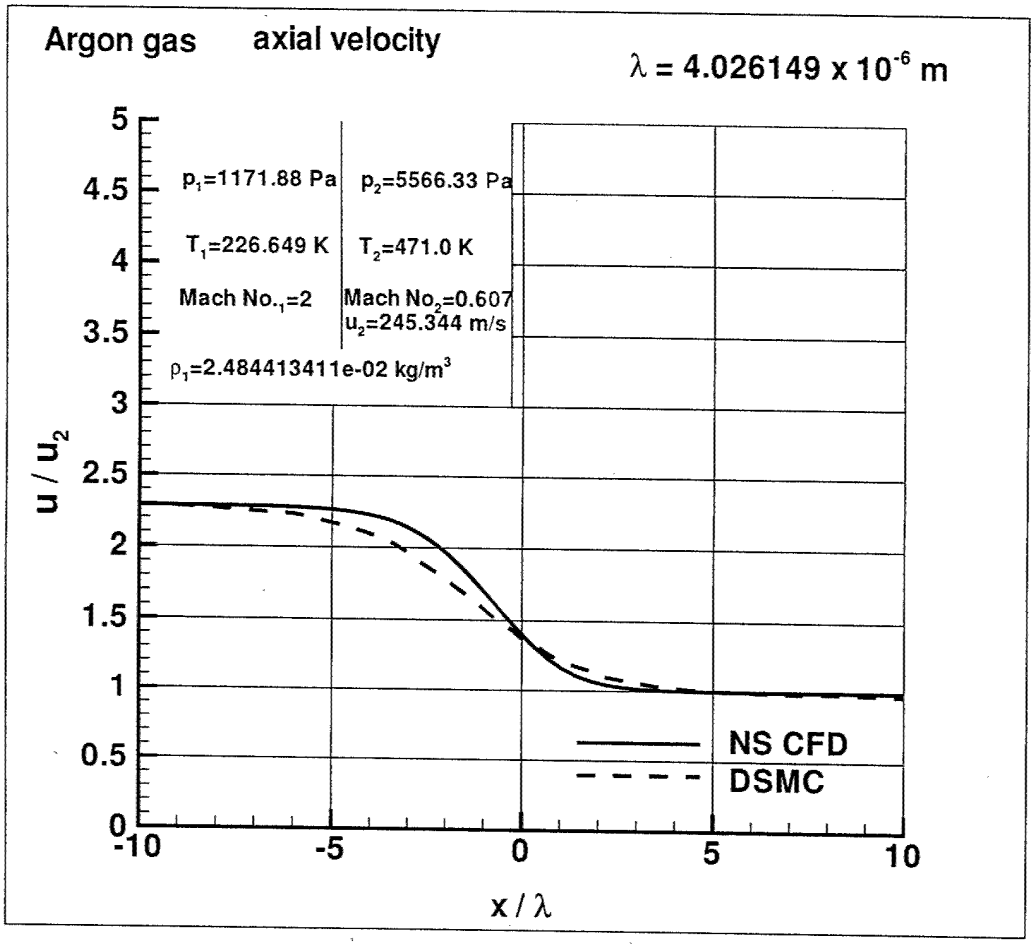

Figure 7: Comparison of velocity across shock wave in Mach 2 argon flow between Navier-Stokes CFD solution and DSMC